Weierstraß-Institut
für Angewandte Analysis und Stochastik

Leibniz-Institut im Forschungsverbund Berlin e. V.

Preprint ISSN 2198-5855

Assessing the quality of the excess chemical potential flux scheme for degenerate semiconductor device simulation

Dilara Abdel, Patricio Farrell, Jürgen Fuhrmann

submitted: November 4, 2020

Weierstrass Institute
Mohrenstr. 39
10117 Berlin
Germany
E-Mail: dilara.abdel@wias-berlin.de
patricio.farrell@wias-berlin.de
juergen.fuhrmann@wias-berlin.de

No. 2787
Berlin 2020

2020 *Mathematics Subject Classification.* 35Q81, 35K57, 65N08.

Key words and phrases. Degenerate semiconductors, drift-diffusion equations, finite volume method, flux discretization, Scharfetter-Gummel scheme.

This work was partially supported by the Leibniz competition.

Edited by
Weierstraß-Institut für Angewandte Analysis und Stochastik (WIAS)
Leibniz-Institut im Forschungsverbund Berlin e. V.
Mohrenstraße 39
10117 Berlin
Germany

Fax: +49 30 20372-303
E-Mail: preprint@wias-berlin.de
World Wide Web: http://www.wias-berlin.de/

Assessing the quality of the excess chemical potential flux scheme for degenerate semiconductor device simulation

Dilara Abdel, Patricio Farrell, Jürgen Fuhrmann

Abstract

The van Roosbroeck system models current flows in (non-)degenerate semiconductor devices. Focusing on the stationary model, we compare the excess chemical potential discretization scheme, a flux approximation which is based on a modification of the drift term in the current densities, with another state-of-the-art Scharfetter-Gummel scheme, namely the diffusion-enhanced scheme. Physically, the diffusion-enhanced scheme can be interpreted as a flux approximation which modifies the thermal voltage. As a reference solution we consider an implicitly defined integral flux, using Blakemore statistics. The integral flux refers to the exact solution of a local two point boundary value problem for the continuous current density and can be interpreted as a generalized Scharfetter-Gummel scheme. All numerical discretization schemes can be used within a Voronoi finite volume method to simulate charge transport in (non-)degenerate semiconductor devices. The investigation includes the analysis of Taylor expansions, a derivation of error estimates and a visualization of errors in local flux approximations to extend previous discussions. Additionally, drift-diffusion simulations of a p-i-n device are performed.

1 Introduction

The standard drift-diffusion model for semi-classical charge transport of free electrons and holes due to a self-consistent electric field in a semiconductor device is the van Roosbroeck system. We consider Voronoi finite volume schemes for the discretization of the semiconductor device equations. We are interested in the numerically more challenging degenerate case and pay particular attention to the choice of flux approximations. One of the most classical numerical flux scheme is arguably the Scharfetter-Gummel scheme [14], which yields a numerical stable and thermodynamically consistent numerical flux, but cannot be used for general charge carrier statistics. A generalization of the Scharfetter-Gummel scheme is available [5], but computationally expensive. Hence, several thermodynamically consistent numerical flux schemes, which modify this generalization to lower the computational costs, are proposed in the literature [6–8, 13]. We focus on the excess chemical potential scheme [16] which appears to be used in parts of the device simulation community. However, unfortunately, there seem to be no direct comparisons of this scheme with other recent modified Scharfetter-Gummel schemes. This paper aims to fill this gap by comparing it to the diffusion enhanced scheme [2], where the integral flux by Eymard et al. is used as a reference flux. It supplements previously made temperature-dependent observations [11].

DOI 10.20347/WIAS.PREPRINT.2787 Berlin 2020

2 Van Roosbroeck model

The stationary variant of the van Roosbroeck system is given by

$$-\nabla \cdot (\varepsilon_s \nabla \psi) = q\Big((p - N_A) - (n - N_D)\Big), \tag{1a}$$

$$\nabla \cdot \mathbf{j}_n = qR(n,p), \tag{1b}$$

$$\nabla \cdot \mathbf{j}_p = -qR(n,p), \tag{1c}$$

where q denotes the elementary charge, ε_s the dielectric permittivity, N_A and N_D describe the density of singly ionized acceptor and donor atoms, and R the recombination. The set of unknowns is expressed by the electrostatic potential ψ and the quasi Fermi potentials for electrons φ_n and holes φ_p. The current densities in the continuity equations (1b) and (1c) are given by

$$\mathbf{j}_n = -q\mu_n n \nabla \varphi_n, \qquad \mathbf{j}_p = -q\mu_p p \nabla \varphi_p, \tag{2}$$

where the electron and hole densities n and p are defined by

$$n = N_c \mathcal{F}(\eta_n), \qquad \eta_n = \frac{q(\psi - \varphi_n) - E_c}{k_B T}, \tag{3a}$$

$$p = N_v \mathcal{F}(\eta_p), \qquad \eta_p = \frac{q(\varphi_p - \psi) + E_v}{k_B T}. \tag{3b}$$

The strictly monotonously increasing statistics function $\mathcal{F}$ will be discussed later. The conduction and valence band density of states are given by N_c and N_v, the mobilities by μ_n and μ_p and the Boltzmann constant by k_B. The conduction and valence band-edge energies are denoted by E_c and E_v and T refers to the temperature. With help of the generalized Einstein relation it is possible to model the diffusion coefficients D_n and D_p via the the nonlinear diffusion enhancement

$$g(\xi) = \xi(\mathcal{F}^{-1})'(\xi) \tag{4}$$

by (introducing the thermal voltage $U_T = k_B T/q$)

$$D_n = \mu_n U_T g\left(\frac{n}{N_c}\right), \quad D_p = \mu_p U_T g\left(\frac{p}{N_v}\right).$$

With this relation, we can rewrite the electric fluxes (2) into a drift-diffusion form

$$\mathbf{j}_n = -q\mu_n n \nabla \psi + qD_n \nabla n, \quad \mathbf{j}_p = -q\mu_p p \nabla \psi - qD_p \nabla p. \tag{5}$$

In general, inorganic semiconductor devices can be modeled by choosing the Fermi-Dirac integral of order one-half [15] for the statistics function $\mathcal{F}$. Non-degenerate semiconductors are modeled with the Boltzmann approximation $\mathcal{F}(\eta) = \exp(\eta)$. In this case, the diffusion enhancement (4) is equal to one. In this work, we focus on degenerate semiconductors, i.e. nonlinear diffusive problems. To compare our flux approximations, we choose the Blakemore statistics [3] function $\mathcal{F}(\eta) = (\exp(-\eta) + \gamma)^{-1}$ with $\gamma = 0.27$ for which an expensive but accurate numerical flux is known [12]. The different statistics with the corresponding diffusion enhancements are depicted in Figure 1. For brevity, we consider only the current density for electrons from now on and will partially omit the index n.

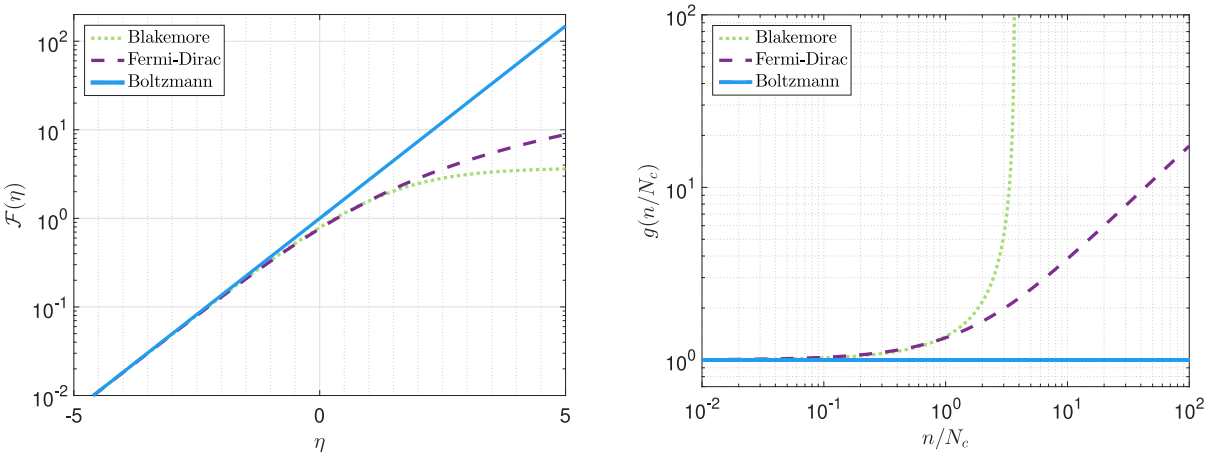

Figure 1: Left: Semi-logarithmic plot of different statistics functions $\mathcal{F}$ for $-5 \leq \eta \leq 5$. Right: Corresponding logarithmic plot of the diffusion enhancement g in (4). This function can be seen as a measure of how far away we are from the Boltzmann regime.

3 Scharfetter-Gummel type fluxes

The open, bounded domain $\mathbf{\Omega}$, on which the model (1) is defined, is partitioned into N control volumes $\boldsymbol{\omega}_K$ such that $\mathbf{\Omega} = \bigcup_{K=1}^{N} \boldsymbol{\omega}_K$, where each $\boldsymbol{\omega}_K$ is associated with a collocation point $\mathbf{x}_K \in \boldsymbol{\omega}_K$. We are interested in a numerical flux j along the edge connecting the collocation points of two neighboring control volumes $\boldsymbol{\omega}_K$ and $\boldsymbol{\omega}_L$ which is assumed to be aligned with the normal direction with respect to the interface $\boldsymbol{\omega}_K \cap \boldsymbol{\omega}_L$. In the following, a subindex K corresponds to an evaluation of a physical quantity at node $\mathbf{x}_K$ and a subindex L to an evaluation at node $\mathbf{x}_L$, respectively. Integrating (1b) over $\boldsymbol{\omega}_K$, using the Gauss divergence theorem and one point quadrature rules yields the discrete counterpart

$$\sum_{\boldsymbol{\omega}_L \in \mathcal{N}(\boldsymbol{\omega}_K)} |\partial\boldsymbol{\omega}_K \cap \partial\boldsymbol{\omega}_L| j_{n;KL} = q|\boldsymbol{\omega}_K| R(n_K, p_K),$$

where $\mathcal{N}(\boldsymbol{\omega}_K)$ denotes the set of all control volumes neighboring $\boldsymbol{\omega}_K$. The nonlinear flux function $j_{n;KL} = j_{n;KL}(\eta_K, \eta_L, \psi_K, \psi_L)$ approximates the projected flux $\mathbf{j} \cdot \boldsymbol{\nu}_{KL}$ locally along the edge $\partial\boldsymbol{\omega}_K \cap \partial\boldsymbol{\omega}_L$, where $\boldsymbol{\nu}_{KL}$ is the corresponding normal vector along $\partial\boldsymbol{\omega}_K \cap \partial\boldsymbol{\omega}_L$. For details concerning the finite volume method see [6].

Furthermore, one property which holds on a continuous level to avoid unphysical state dissipation is the *preservation of thermodynamic equilibrium* [6]. Mathematically, this means that vanishing fluxes shall imply constant quasi Fermi potentials. A numerical flux $j = j_{KL}$ is now said to be thermodynamically consistent, if it satisfies an analogous discrete relation, i.e.

$$j = 0 \quad \text{implies} \quad \delta\eta_{KL} = \delta\psi_{KL},$$

where $\delta\eta_{KL} = \eta_L - \eta_K$ and $\delta\psi_{KL} = (\psi_L - \psi_K)/U_T$. Thermodynamic consistency is also important, when coupling the van Roosbroeck system to heat transport models [7]. We discuss now different thermodynamically consistent numerical fluxes that may be used within a Voronoi finite volume framework.

3.1 Generalized Scharfetter-Gummel scheme

Under the assumption that the flux $\mathbf{j}_n$ and the electric field $-\nabla\psi$ are constant along each face of a Voronoi cell, the flux can be projected onto the shared edge between two neighboring control volumes. Then, an integral equation can be derived [5], which shall be satisfied by the unknown local numerical flux j

$$\int_{\eta_K}^{\eta_L} \left(\frac{j/j_0}{\mathcal{F}(\eta)} + \delta\psi_{KL} \right)^{-1} d\eta = 1, \quad j_0 = q\mu_n N_c \frac{U_T}{h_{KL}}, \tag{6}$$

where η is defined in (3). The integration limits are given by $\eta_K = \eta_n(\psi_K, \varphi_K)$ and $\eta_L = \eta_n(\psi_L, \varphi_L)$ and h_{KL} denotes the Euclidean distance between two neighboring nodes $\mathbf{x}_K$ and $\mathbf{x}_L$. The existence of a solution to (6) was proven [10], even though the integral equation is in general not explicitly solvable. We refer to the solution of (6) as *generalized* Scharfetter-Gummel flux. Note that for non-degenerate semiconductor devices the generalized scheme reduces to the classical Scharfetter-Gummel scheme [14]

$$j_{sg} = B(\delta\psi_{KL})\, e^{\eta_L} - B(-\delta\psi_{KL})\, e^{\eta_K}, \tag{7}$$

for a non-dimensionalized edge current $j_{sg} = j/j_0$ with B as the Bernoulli function which is defined by $B(x) := x/(e^x - 1)$, $B(0) = 1$. Additionally, it was shown in [12] that for degenerate semiconductors based on Blakemore statistics the integral equation (6) can be reduced to a fixed point equation, namely

$$j_g = B(\delta\psi_{KL} + \gamma j_g)\, \mathrm{e}^{\eta_L} - B\left(-\left[\delta\psi_{KL} + \gamma j_g\right]\right) \mathrm{e}^{\eta_K}. \tag{8}$$

The implicit equation in (8) can be solved within a few Newton steps, but the efficiency of this flux is highly dependent on the choice of initial value. Hence, computationally less expensive flux discretization schemes are needed as an alternative. Still, we will use this scheme as a reference flux for the case of degenerated semiconductors, modeled by Blakemore statistics.

3.2 Diffusion enhanced scheme

Recently, another *modified* Scharfetter-Gummel discretization scheme was introduced [2]. There, a logarithmic average for the nonlinear diffusion enhancement g in (4) is considered,

$$g_{KL} = \frac{\eta_L - \eta_K}{\log \mathcal{F}(\eta_L) - \log \mathcal{F}(\eta_K)}, \tag{9}$$

resulting in the local flux approximation

$$j_d = g_{KL} \left[B\left(\frac{\delta\psi_{KL}}{g_{KL}} \right) \mathcal{F}(\eta_L) - B\left(-\frac{\delta\psi_{KL}}{g_{KL}} \right) \mathcal{F}(\eta_K) \right]. \tag{10}$$

We stress that, in case of a denominator in (9) near zero, i.e. $\eta_K \approx \eta_L$, regularization strategies need to be developed to handle the removable singularity.

3.3 “Sedan” scheme

The earliest reference we could find for the excess chemical potential scheme is the source code of the SEDAN III simulator [16], therefore in the following, we will likewise refer to this scheme as the *Sedan scheme*. There are benchmarks computed by the device simulator SEDAN III itself available in

literature, but to the best of our knowledge there are barely any comparisons of this flux discretization scheme with other schemes known. A numerical analysis focused comparison of this flux approximation is given in [4]. The scheme is motivated by rearranging the drift part in (5) to include the *excess chemical potential*, $\mu^{ex} = \log \mathcal{F}(\eta) - \eta$, yielding

$$j_s = B\left(Q_{KL}\right)\mathcal{F}(\eta_L) - B\left(-Q_{KL}\right)\mathcal{F}(\eta_K) \tag{11}$$

with

$$Q_{KL} = \delta\psi_{KL} + \mu_L^{ex} - \mu_K^{ex} = \delta\psi_{KL} - (\eta_L - \eta_K) + \log\frac{\mathcal{F}(\eta_L)}{\mathcal{F}(\eta_K)}. \tag{12}$$

4 Comparison of flux discretizations

This paper aims to extend a previous discussion [7] by examining similar aspects for the excess chemical potential flux approximation introduced in Section 3.3.

4.1 Taylor expansions

Taylor expansions of the following form dependent on $\delta\psi_{KL}$ and $\delta\eta_{KL}$

$$\begin{aligned} j_k = &-\mathcal{F}(\bar{\eta}_{KL})\delta\psi_{KL} + \mathcal{F}(\bar{\eta}_{KL})\delta\eta_{KL} \\ &+ \alpha_1\delta\psi_{KL}^2\delta\eta_{KL} + \alpha_2\delta\psi_{KL}\delta\eta_{KL}^2 + \alpha_3\delta\eta_{KL}^3, \quad k \in \{g, s, d\}, \end{aligned} \tag{13}$$

can be derived for the flux approximations introduced in Section 3, when expanding in $\bar{\eta}_{KL} = (\eta_L + \eta_K)/2$, see [1] and [7]. For the prefactors α_j, $j \in \{1, 2, 3\}$, we have

$$\alpha_j = \alpha_j\Big(\mathcal{F}(\bar{\eta}_{KL}), \mathcal{F}'(\bar{\eta}_{KL}), \mathcal{F}''(\bar{\eta}_{KL}), \mathcal{F}'''(\bar{\eta}_{KL})\Big).$$

The absolute error in these prefactors α_j between the Taylor expansions of the generalized Scharfetter-Gummel scheme and the two modified ones is depicted in Figure 2.

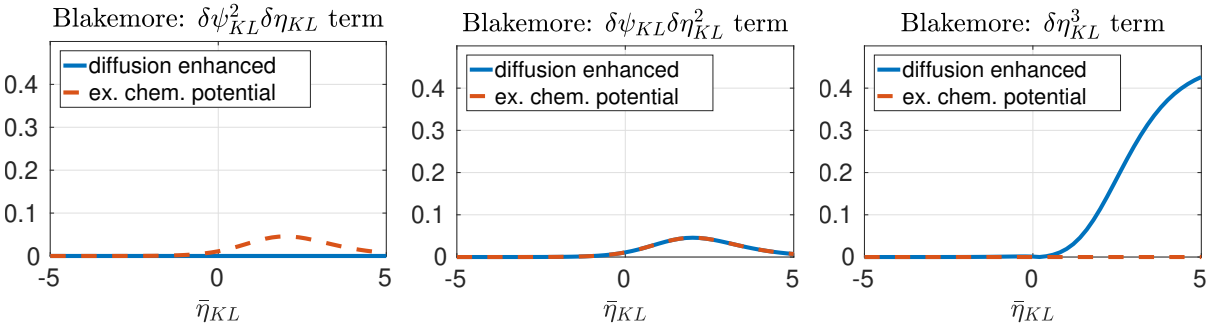

Figure 2: Errors between the third-order prefactors of Taylor series expansion of the exact Scharfetter-Gummel scheme (6) and the two modified schemes for $\bar{\eta}_{KL} \in [-5, 5]$.

For large negative arguments of the function $\mathcal{F}$ the Boltzmann and the Blakemore statistics nearly coincide, corresponding to the non-degenerate case. Hence, the modified Scharfetter-Gummel schemes converge towards the classical scheme (7) and we observe nearly vanishing errors in Figure 2. For large positive arguments we observe that the errors in the prefactors corresponding to the diffusion

enhanced scheme increase with the exponents of $\delta\eta_{KL}$, whereas the error corresponding to the excess chemical potential scheme nearly vanishes. Due to this observation it gives rise to think that in case of no electrical field the excess chemical potential flux performs better than the diffusion enhanced scheme. However, neither the diffusion enhanced nor the excess chemical potential scheme is third-order accurate. To measure the quality of the fluxes in a different manner, second-order error estimates for the local flux errors are considered next.

When neglecting third-order terms, the following error bounds between the modified and the generalized flux dependent on the diffusion enhancement can be derived [1, 7]

$$|j_s - j| \leq \frac{1}{2}\frac{\mathcal{F}(\bar{\eta}_{KL})}{g(\bar{\eta}_{KL})}\Big(|\delta\psi_{KL}\delta\eta_{KL}| + \delta\eta_{KL}^2\Big), \tag{14}$$

$$|j_d - j| \leq \frac{1}{2}\frac{\mathcal{F}(\bar{\eta}_{KL})}{g(\bar{\eta}_{KL})}|\delta\psi_{KL}\delta\eta_{KL}|. \tag{15}$$

The error bounds indicate a better performance of the diffusion enhanced scheme for large values of the diffusion enhancement g, i.e. for statistics strongly deviating from the Boltzmann regime.

4.2 Error between local flux approximations

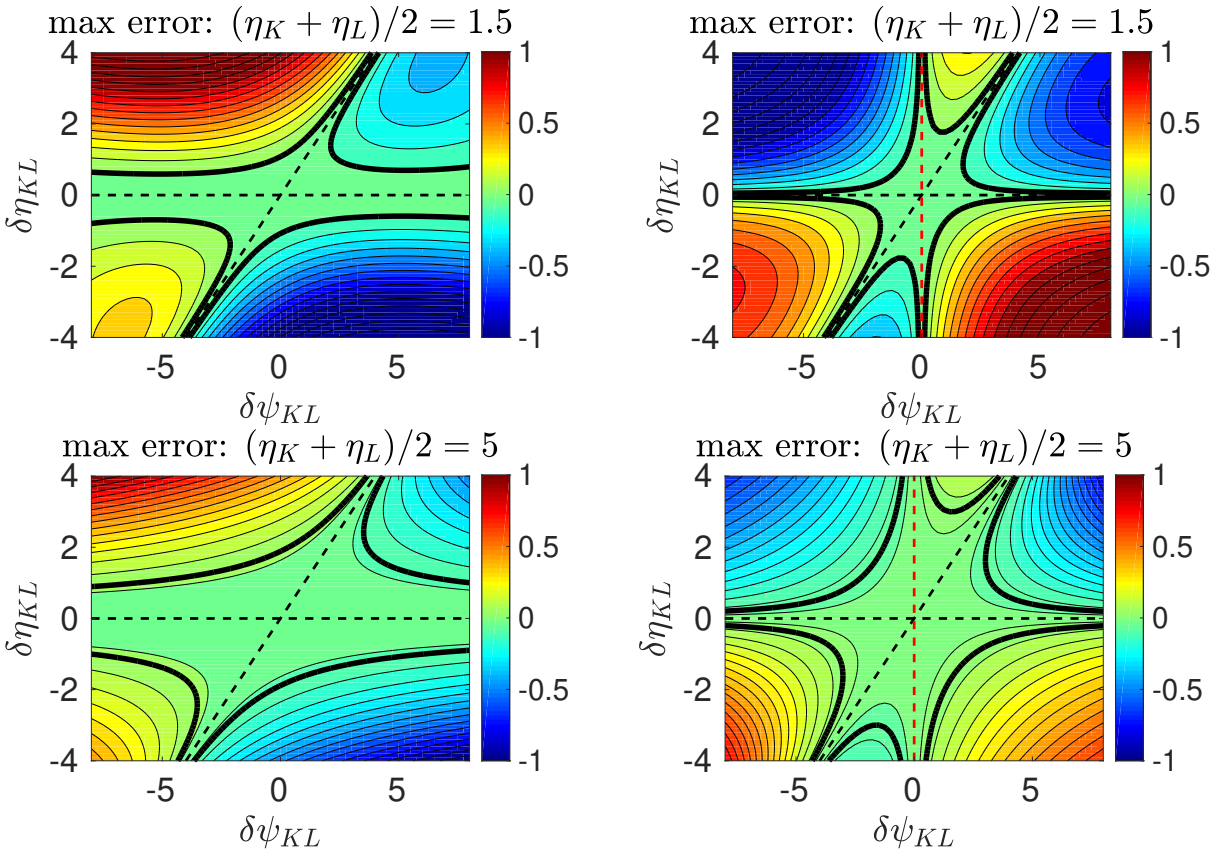

Figure 3: Logarithmic absolute errors between the Taylor expansions of the generalized Scharfetter-Gummel and the diffusion enhanced scheme (left) and the excess chemical potential scheme (right) for two fixed averages $\bar{\eta}_{KL} = 1.5$ and $\bar{\eta}_{KL} = 5$.

We study the logarithmic error between the modified flux schemes and the generalized scheme for two fixed averages $\bar{\eta}_{KL}$. The errors for the simulation of a degenerate semiconductor can be seen in Figure

3. The black dashed lines correspond to thermodynamic consistency, as well as pure drift currents, i.e. $\eta_K = \eta_L$. In both cases, the modified schemes agree exactly with the generalized scheme.

Since $\mathcal{F}(\bar{\eta}_{KL})/g(\bar{\eta}_{KL}) = \mathcal{F}'(\bar{\eta}_{KL})$, the derivative of the statistics function appears in the error estimates (14) and (15). The derivative of the Blakemore statistics decreases for large positive arguments. Hence, we observe in Figure 3 that increasing the average $\bar{\eta}_{KL}$ results in a comparatively smaller error. Both, the error estimates (14), (15) and Figure 3 indicate a larger area, where the diffusion enhanced and the generalized scheme agree well for small values of $\delta\eta_{KL}$ and large values of the potential difference $\delta\psi_{KL}$. Further, the red dashed line in Figure 3 indicates agreement of the excess chemical potential scheme and the exact solution of (6) for a purely diffusive flux $\mathbf{j}$, i.e. a vanishing electrical field $\delta\psi_{KL} = 0$. This can be proven analytically, see [1]. In this specific case, the excess chemical potential scheme is the best possible flux approximation.

5 Numerical example

Finally, we study the impact of the different flux discretization schemes on the simulation of degenerate semiconductor devices for a 6μm long GaAs p-i-n diode with a width of 0.5μm and a depth of $1.0 \cdot 10^{-4}$cm. On each 2μm long layer we choose $N = 3 \cdot 2^{n_{ref}-1}$ uniform nodes. The open source Julia-based solver `ChargeTransportInSolids`, based on `VoronoiFVM` [9] was used which allows to use automatic differentiation. The stationary van Roosbroeck system (1) with zero recombination supplemented with Dirichlet-Neumann boundary conditions is considered. The resulting current voltage curves for a refinement level $n_{ref} = 3$ and the L^∞ errors in the computed total currents based on the different flux approximations for the first nine refinement level are depicted in Figure 4. It can be observed that eventually the errors in the computed total currents based on the flux schemes converge with order $\mathcal{O}(h^2)$. Furthermore, it suggests that on coarse meshes, which are hard to avoid for expensive 3D simulations, the excess chemical potential flux performs better than the diffusion enhanced scheme.

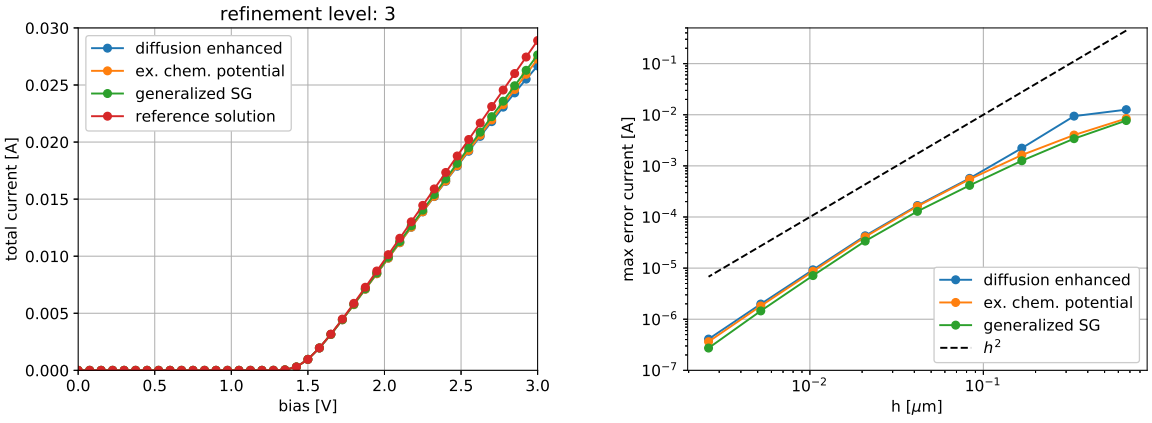

Figure 4: Left: The I-V curves computed with the different schemes for fixed mesh refinement. The reference solution was computed using the generalized Scharfetter-Gummel scheme on refinement level 10. Right: Convergence studies for the absolute errors of the total currents.

6 Conclusion

Our goal was to assess the quality of the Sedan flux (11) which has received surprisingly little attention in the literature. To this end, we compared it to another modified Scharfetter-Gummel scheme (10) by studying its error with respect to the more accurate but expensive integral flux (6). For this, we analyzed Taylor expansions of the flux discretization schemes, the errors in the local flux approximations and simulated a p-i-n benchmark. Further applications of this scheme will be part of future research.

References

[1] D. Abdel. Comparison of flux discretizations for generalized drift-diffusion systems. Master's thesis, Technical University Berlin, 2020.

[2] M. Bessemoulin-Chatard. A finite volume scheme for convection-diffusion equations with nonlinear diffusion derived from the scharfetter-gummel scheme. *Numer. Math.*, 121:637–670, 2012.

[3] J. S. Blakemore. The parameters of partially degenerate semiconductors. *Proceedings of the Physical Society. Section A*, 65:460–461, 1952.

[4] C. Cancès, C. Chainais-Hillairet, J. Fuhrmann, and B. Gaudeul. A numerical-analysis-focused comparison of several finite volume schemes for a unipolar degenerate drift-diffusion model. *IMA Journal of Numerical Analysis*, 07 2020. DOI: 10.1093/imanum/draa002.

[5] R. Eymard, J. Fuhrmann, and K. Gärtner. A finite volume scheme for nonlinear parabolic equations derived from one-dimensional local dirichlet problems. *Numer. Math.*, 102:463–495, 2006.

[6] P. Farrell, D. H. Doan, M. Kantner, J. Fuhrmann, T. Koprucki, and N. Rotundo. Drift-diffusion models. In *Optoelectronic Device Modeling and Simulation: Fundamentals, Materials, Nanostructures, LEDs, and Amplifiers*, pages 733–771. CRC Press Taylor & Francis Group, 2017.

[7] P. Farrell, T. Koprucki, and J. Fuhrmann. Computational and analytical comparison of flux discretizations for the semiconductor device equations beyond boltzmann statistics. *J. Comput. Phys.*, 346:497–513, 2017.

[8] P. Farrell, M. Patriarca, J. Fuhrmann, and T. Koprucki. Comparison of thermodynamically consistent charge carrier flux discretizations for Fermi–Dirac and Gauss–Fermi statistics. *Opt Quant Electron*, 50:101, 2018.

[9] J. Fuhrmann. VoronoiFVM.jl - Solver for coupled nonlinear partial differential equations based on the Voronoi finite volume method. `https://github.com/j-fu/VoronoiFVM.jl`, 2019. DOI: 10.5281/zenodo.3529808.

[10] K. Gärtner. Existence of bounded discrete steady-state solutions of the van Roosbroeck system with monotone Fermi–Dirac statistic functions. *Journal of Computational Electronics*, 14(3):773–787, 2015.

[11] M. Kantner. Generalized scharfetter–gummel schemes for electro-thermal transport in degenerate semiconductors using the kelvin formula for the seebeck coefficient. *Journal of Computational Physics*, 402:109091, 2020.

[12] T. Koprucki and K. Gärtner. Discretization scheme for drift-diffusion equations with strong diffusion enhancement. *Opt. Quant. Electronics*, 45:791–796, 2013.

[13] M. Patriarca, P. Farrell, T. Koprucki, and M. Auf der Maur. Highly accurate discretizations for non-boltzmann charge transport in semiconductors. pages 53–54, 11 2018.

[14] D. L. Scharfetter and H. K. Gummel. Large-signal analysis of a silicon read diode oscillator. *IEEE Transactions on Electron Devices*, 16(1):64–77, 1969.

[15] S. M. Sze and K. K. Ng. *Physics of Semiconductor Devices*. Wiley, 2006.

[16] Z. Yu and R. Dutton. SEDAN III – A one-dimensional device simulator. `www-tcad.stanford.edu/tcad/programs/sedan3.html`, 1988.